

# Crystallization Behavior of Poly(ether ether ketone ketone)

JUNZUO WANG,<sup>1,\*</sup> JUNKUI CAO,<sup>1</sup> YAN CHEN,<sup>1</sup> YANGCHUAN KE,<sup>1</sup> ZHONGWEN WU,<sup>1</sup> and ZHISHEN MO<sup>2</sup>

<sup>1</sup>Department of Chemistry, Jilin University, Changchun 130023, and <sup>2</sup>Changchun Institute of Applied Chemistry, Academia Sinica, Changchun 130021, People's Republic of China

## SYNOPSIS

The melting behavior of semicrystalline poly(ether ether ketone ketone) (PEEKK) has been studied by differential scanning calorimetry (DSC). When PEEKK is annealed from the amorphous state, it usually shows two melting peaks. The upper melting peaks arise first, and the lower melting peaks are developed later. The upper melting peaks shown in the DSC thermogram are the combination (addition) of three parts: initial crystal formed before scanning; reorganization; and melting–recrystallization of lower melting peaks in the DSC scanning period. In the study of isothermal crystallization kinetics, the Avrami equation was used to analyze the primary process of the isothermal crystallization; the Avrami constant,  $n$ , is about 2 for PEEKK from the melt and 1.5 for PEEKK from the glass state. According to the Lauritzen–Hoffman equation, the kinetic parameter of PEEKK from the melt is 851.5 K; the crystallization kinetic parameter of PEEKK is higher than that of PEEK, and suggests the crystallizability of PEEKK is less than that of PEEK. The study of crystallization on PEEKK under nonisothermal conditions is also reported for cooling rates from 2.5°C/min to 40°C/min, and the nonisothermal condition was studied by Mandelkern analysis. The results show the nonisothermal crystallization is different from the isothermal crystallization. © 1996 John Wiley & Sons, Inc.

## INTRODUCTION

Since the introduction of the high-performance engineering plastics, the commercial semicrystalline poly(aryl ether ketone)s, they have rapidly attracted peoples' attention. Many large chemical corporations have developed different poly(aryl ether ketone)s, which include poly(ether ether ketone) (PEEK), poly(ether ketone) (PEK; ICI), poly(ether ether ketone ketone) (PEEKK; HOECHST), poly(ether ketone ether ketone ketone) (PEKEKK; BASF), etc. PEEKK is a member of the poly(aryl ether ketone) family, its glass transition temperature is 159°C, and the melting point is 360°C. The crystal structure of PEEKK has been studied and reported<sup>1</sup>; PEEKK has the same crystal structure as PEEK. The orthorhombic cell parameters are  $a = 7.75 \text{ \AA}$ ,  $b$

$= 6.00 \text{ \AA}$ ,  $c = 10.10 \text{ \AA}$ ,  $V = 470 \text{ \AA}^3$ ,  $P_c = 1.385 \text{ g cm}^{-3}$ . The crystallinity is 37.5% by wide-angle X-ray diffraction when PEEKK is treated at 320°C. The heat of fusion of the PEEKK perfect crystal was assumed to be 124 J/g.<sup>1</sup> The different thermal histories and processing conditions deeply affect its crystallinity and final property. PEEKK crystalline samples can be obtained by cooling the melt or by isothermal crystallization at temperatures between the  $T_g$  and  $T_m$  from the rubbery state and the melt.<sup>2-3</sup> In this study we have used differential scanning calorimetry to measure the heat flow during crystallization. The Avrami equation was used to analyze the isothermal crystallization during the primary crystallization process. A study of crystallization on PEEKK under nonisothermal conditions is reported for cooling rates from 2.5°C/min to 40°C/min; the nonisothermal condition was studied by Mandelkern analysis.<sup>4</sup> The effect of thermal history, crystallization temperature and time, and scanning rates on PEEKK crystallization melting behavior were also investigated in this paper.

\* To whom correspondence should be addressed at the Department of Chemistry, Jilin University, 119 Jie Fang Rd., Changchun 130023, PRC.

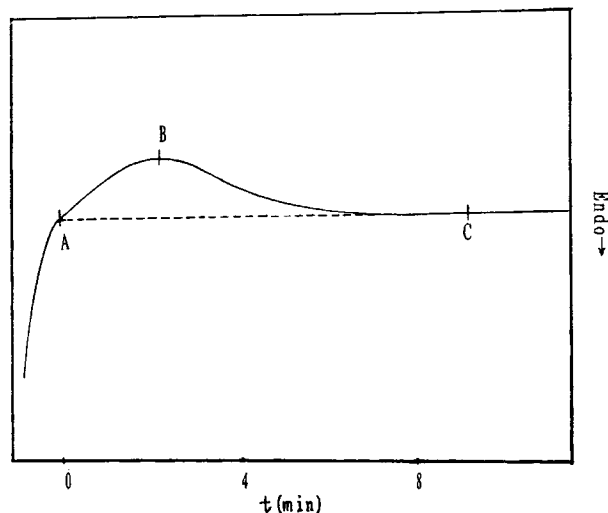


**Figure 1** Heat flow vs. time during isothermal crystallization at 317°C.

## EXPERIMENTAL

Samples used in the study were prepared from 1,4-bis(4'-fluorobenzoyl)benzene and hydroquinone.<sup>5,6</sup> The inherent viscosity is 1.07 dL/g when measured in 98% H<sub>2</sub>SO<sub>4</sub> (at 25°C 0.01 g/10 mL concentration). The PEEKK powder was pressed at 410°C under 10 MPa pressure for 5 min, then quenched into an ice-water bath to form thin 0.3 mm amorphous PEEKK film. Wide-angle X-ray diffraction measurement indicated that the PEEKK film was completely amorphous; the thermal treatment samples can be prepared by annealing the amorphous films at various temperatures for predetermined periods of time and then putting them into an ice/water mixture. A DuPont 2000 thermal analyzer was used to monitor the heat flow from the sample during crystallization. Isothermal crystallization was brought to completion by heating the amorphous films above the glass transition temperature (182–186°C). The high temperature crystallization was carried out by first heating the sample to 410°C for 10 min to melt it, then fast-cooling to the isothermal crystallization temperature. Figure 1 presents the heat flow change for isothermal crystallization at 317°C. Crystallization begins at A, the maximum is reached at B, the crystallization slows down beyond B, and the measurement is terminated when no more heat flows from the sample. The relative degree of crystallinity as a function of time,  $X_c(t)$  was found from  $X_c(t)/X_c(\infty) = \int_0^t Q(t) dt$ , where  $X_c(\infty)$  is the ultimate crystallinity at very long time, and  $Q(t)$  is the heat flow rate.  $X_c(\infty)$  was found from the heat flow of the isothermally crystallized samples.

## RESULTS AND DISCUSSION

### Effect of Thermal History on PEEKK Crystallization and Melting Behavior

The amorphous PEEKK was scanned at 10°C/min heating rate, as shown in Figure 2. The curve shows a sharp exothermic peak at 191°C after the glass transition at 159°C, its heat flow is 19.67 J/g, a broad endotherm with a peak at 360.2°C, and the enthalpy change is 33.34 J/g. The large difference between endothermic peak area and exothermic peak area cannot be an instrumental error. This phenomenon is similar to PET, which is the result of the crystallization in the DSC scanning period.<sup>7,8</sup> Amorphous PEEKK can crystallize above  $T_g$  and there is a sharp exotherm from 180°C to 220°C. Even above 220°C, the PEEKK can still crystallize as the lamellae gradually thicken and become perfect. This is a crystallization reorganization process. The crystallization exotherm is too gradual to investigate in the thermogram; however, we did not eliminate the formation of new crystals and growth in this process. Therefore, the PEEKK can crystallize throughout the whole DSC scanning process.

In order to gain further insight into the crystallization melting behavior of PEEKK, we treat PEEKK samples by means of rapid dynamic thermal cycling.<sup>9</sup> The results are given in Figure 3. The amorphous PEEKK sample was quickly heated to 215°C (see curve *a* in Fig. 3), then fast-cooled to room temperature and scanned to 245°C at 20°C/min heating rate (see curve *b* in Fig. 3), then next fast-cooled and reheated to 295°C (curve *c* in Fig. 3), the sample was finally scanned to 400°C, and curve *d* in Figure 3 was obtained. Curve *a* is identical to that in Figure 2 up to 215°C. In curve *b*, we find a small endotherm at 227°C, followed immediately by a crystallization exotherm that indicated a crys-

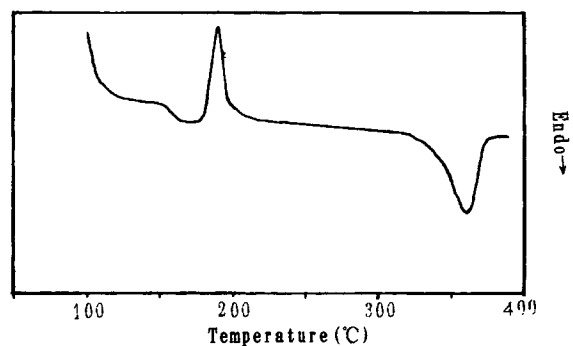


**Figure 2** DSC scans (10°C/min) of amorphous PEEKK.

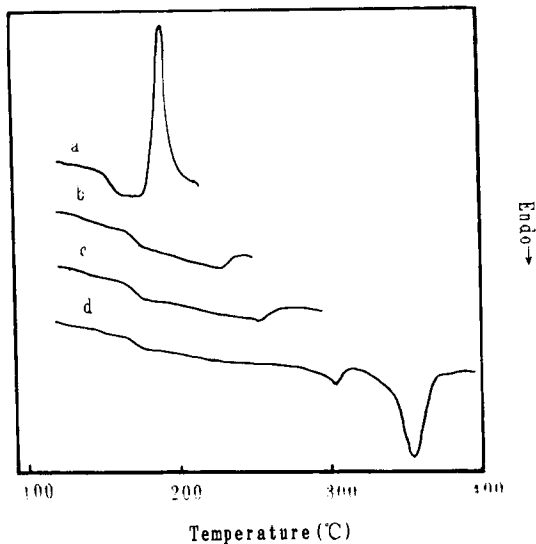


**Figure 3** DSC scans at 20°C/min for PEEKK by a dynamic cycling experiment (a) the amorphous film was heated to 215°C at 20°C/min (curve a) then quickly cooled to room temperature and scanned to 245°C at 20°C/min (curve b), cooled and reheated to 295°C at 20°C/min (curve c), cooled and reheated to 400°C at 20°C/min (curve d).

tallization melting and recrystallization process. In curve *c* and curve *d*, the endothermic peaks appear at 256°C and 305°C, and the exothermic peak becomes unclear with the increasing of the temperature; moreover, the endothermic peak becomes narrower and the area becomes larger as the scanning temperature increases. We could not find former endothermic effects occurring near 227°C and 256°C in curve *c* and curve *d*. In other words, the lower melting peaks in the later thermal cycling had transformed into more perfect crystals by a continuous melting and recrystallization process. Recently, A. M. Jonas<sup>10</sup> found melting and recrystallization when the semicrystalline PEEK and PET samples were heated above the previous highest annealing temperatures; therefore, the low temperature crystallization becomes more perfect with the increasing of the thermal treatment temperatures and times of thermal cycling.

#### Effect of Thermal Treatment Temperature and Time on PEEKK Crystallization Melting Behavior

Amorphous PEEKK samples were annealed for 6 h at 225°C, 250°C, 280°C, 300°C, and 350°C, respectively. Then they were scanned at 10°C/min heating rate as shown in Figure 4. Every sample had two

melting peaks, the upper melting peak was about 360°C regardless of heat treatment temperature, while the lower melting peak is 10–15°C higher than the corresponding heat treatment temperature. When the heat treatment temperature was high enough (350°C), the two peaks became a single peak.

Amorphous PEEKK samples were annealed at 250°C for 15 min, 30 min, 60 min, 150 min, and 300 min, respectively, then scanned at a 10°C/min heating rate. The lower melting peak ( $T_{m1}$ ) and its heat flow ( $\Delta H_1$ ), upper melting peak ( $T_{m2}$ ), and its heat flow ( $\Delta H_2$ ), are listed in Table I. The longer the heat treatment time, the higher the lower melting peak and the more its heat flow, while there is little change to upper melting peak and its heat flow. We think the double peaks are the results of the melting of crystal populations with two different degrees of perfection,<sup>9,11,12</sup> the upper melting peak relating to the melting of main crystal population first developed on the heat treatment crystallization, while the smaller area developed later. The high-temperature crystallization is completed quickly because of rapid nucleation, from Table I, and the  $\Delta H_2$  relating to upper melting peak is unchanged when thermal treatment time is above 15 min; the lower temperature melting peak formed after the large crystalline lamellae (upper melting peak), and were limited by the large lamellae, along with the development of temperature and time; small crystals thickened and reorganized into more perfect crystallines, hence,  $T_{m1}$  and  $\Delta H_1$  become greater with increasing time.

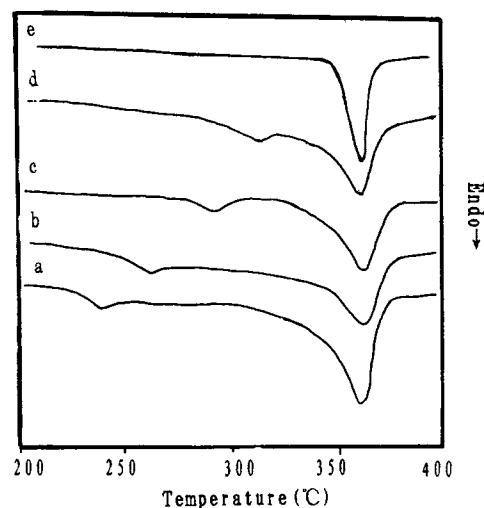


**Figure 4** DSC scans at 10°C/min of PEEKK films annealed for 6 h at (a) 225°C (b) 250°C (c) 280°C (d) 300°C (e) 350°C.

**Table I Effect of the Different Thermal Treatment Times at 250°C on the Crystallization Melting Behavior of PEEKK**

No.	Time (min)	$T_{m1}$ (°C)	$T_{m2}$ (°C)	$\Delta H1$ (J/g)	$\Delta H2$ (J/g)
1	15	259.72	359.65	1.149	36.24
2	30	260.36	360.11	1.228	36.05
3	60	261.60	360.50	1.620	36.56
4	150	264.04	360.57	1.956	36.72
5	300	268.25	360.72	2.193	36.42

### Effect of Heating Rate on PEEKK Crystallization Melting Behavior

Table II describes separately that amorphous PEEKK was annealed for a long time (6 h) at 250°C and 300°C, then scanned at the rate of 2°C/min, 5°C/min, 10°C/min, and 20°C/min. The same results showed that the lower melting peak improves and the upper melting peak declines with the increase of heating rate. This phenomenon is also found in PEEK, PPS, PET, etc.<sup>7,8,13-18</sup> It is general among semicrystalline polymers with crystalline defects. We have just discussed that double endotherms were the result of the melting of the crystal population with different degrees of perfection, and could be molten to a single peak under certain conditions (heat treatment at 350°C). These results were also achieved by dynamic heat treatment (DSC scanning). In the amorphous PEEKK DSC measurement, we have known that PEEKK can crystallize in the DSC scanning process. In addition, according to the dynamic thermal cycling experiment, the lower melting peak may transform into an upper melting peak by a continuous melting-recrystallization period. Therefore, the upper melting peak shown in the DSC thermogram is the combination (or addition) of three parts: initial crystal formed before scanning, the crystallization reorganization, and melting-recrystallization of the lower melting peak in the DSC scanning period. The initial crystal is similar because of the same heat treatment temperature and time, while in the DSC scanning process the time of crystallization reorganization and melting-recrystallization is different. The time of crystallization reorganization and melting-recrystallization became shorter as the scanning rate increased; the final upper melting peaks are the crystallization melting of thick lamellae, which formed in the isothermal heat treatment process and DSC scanning process because of crystallization reorganization and melting-recrystallization. Therefore, when the scanning rate is faster, the time of

crystallization reorganization and melting-recrystallization is shorter and the final crystallization perfection degree is less; hence, the upper melting peak will appear at the lower temperature. On the contrary, when the scanning rate becomes slower, it has enough time to reorganize and recrystallize, and the final endothermic peak will appear at a high temperature. However, the upper melting peak has no influence on the lower melting peak, and with the increasing scanning rate, that is only a result of a superheating phenomenon. Therefore, the essence of multi-melting peaks from the cold crystallization is the melting of crystal populations with different degrees of perfection. The effect of the crystallization reorganization and melting-recrystallization in the DSC scanning process on the upper melting peak should be considered.

### Isothermal Crystallization Kinetics of PEEKK

Table III presents the results of crystallinity and time for isothermal crystallization from the melt and rubbery-amorphous state. During the high temperature (309–317°C) isothermal crystallization, though the crystallization rates become slower with the increasing of the crystallization temperature,  $t_{max}$ , and relative degree of crystallinity [ $X_c(t_{max})/X_c(\infty)$ ] become larger as the crystallization temperature increased. The final absolute degree of crystallinity does not change. According to the comparison of the melting isothermal crystallization period and rubbery isothermal crystallization period, the absolute degree of crystallinity for the high temperature crystallization is slightly higher than for crystallization from the glass state, though the final crystallization time of the rubbery state is shorter than that of the high temperature crystallization. The relative amount of degree of crystallinity has been plotted in Figure 5 for the six crystallization temperatures. The relative crystallization can be analyzed using the Avrami equation<sup>19</sup>

**Table II** Effect of Scanning Rates on the Melting Peaks

Scanning Rate (°C/min)	$T_c = 225^\circ\text{C}$		$T_c = 300^\circ\text{C}$	
	$T_{m1}$ (°C)	$T_{m2}$ (°C)	$T_{m1}$ (°C)	$T_{m2}$ (°C)
2	236.4	362.8	307.1	362.6
5	237.4	362.1	311.2	361.1
10	240.0	360.4	311.8	359.7
20	242.2	359.8	314.6	359.3

$$X_c(t)/X_c(\infty) = 1 - \exp(-kt^n) \quad (1)$$

$$\ln[1 - X_c(t)/X_c(\infty)] = -kt^n \quad (2)$$

$$\begin{aligned} \text{or } \log[-\ln(1 - X_c(t)/X_c(\infty))] \\ = n \log t + \log k \quad (3) \end{aligned}$$

where  $n$  is a constant whose value depends on the mechanism of nucleation and form of crystal growth, and  $k$  is a constant containing the nucleation and growth parameters. Plots of  $\log\{-\ln[1 - X_c(t)/X_c(\infty)]\}$  versus  $\log t$  are shown in Figure 6. Each curve has a linear portion followed by a gentle roll-off at longer time. In Figure 6, the deviation from the linear relationship becomes greater at the increasing crystallization rates. In other words, the lower the isothermal crystallization temperature is, the faster the primary crystallization transforms to the secondary crystallization. We guess it has more imperfect crystallization (secondary crystallization) with the increasing of the crystallization rates and spherulitic collision. Fitting the initial linear portion of  $\log\{-\ln[1 - X_c(t)/X_c(\infty)]\}$  versus  $\log t$ , we obtain  $n$  of about 2 for the high-temperature crystallization and 1.5 for the rubbery crystallization. We use eq. (2) and  $d^2X/dt^2$  to obtain

$$t_i = [(n - 1)/nk]^{1/n} \quad (4)$$

We calculated values of  $t_i$  through eq. (4) and listed them in Table IV. These values can be compared with the  $t_{\max}$  obtained from Table III. The agreement in  $t_i$  values suggests that the Avrami analysis works well in describing the initial crystallization process. We scanned the samples which had just finished the isothermal crystallization process. The thermogram shows the double peaks phenomenon just as in PEEK.<sup>15,16</sup> The lower temperature peak is about 10°C higher than the isothermal crystallization temperature; the higher temperature peak increases with the increasing of the isothermal crystallization temperature. Making use of the Hoffman-Weeks<sup>20</sup> equation, we can approximately calculate the equilibrium melting point: the value is 387°C; that is very similar to those K. Könnecke reported<sup>2</sup> ( $T_m^0 = 385^\circ\text{C}$ ) in the DSC method. If we assume that PEEKK crystallization at high temperature follows the Lauritzen-Hoffman equation,<sup>21</sup> we can write the growth equation

$$G = G_0 \exp[-U/R(T - T_\infty)] \times \exp[-K_g T_m^0 / T \Delta T f] \quad (5)$$

$$K_g = 4b\sigma\sigma_e / \Delta Hk \quad (6)$$

In this equation,  $U$  is the transport activation energy; we chose  $U$  equal to 8.38 kJ/mol,<sup>9,13</sup> and  $T_m^0$

**Table III** Crystallinity and Time Data for Isothermal Crystallization from the Melt (309–317°C) and Rubbery Amorphous State (182–186°C)

$T_c$ (°C)	$t_{\max}$ (min)	$t_c$ (min)	$X_c(\infty)$ (%)	$X_c(t_{\max})/X_c(\infty)$
309	0.62	6.72	27	0.28
311	1.00	9.10	27	0.32
315	1.53	9.18	27	0.34
317	2.11	9.27	25	0.44
182	0.16	4.23	20	0.27
186	0.14	3.53	23	0.24

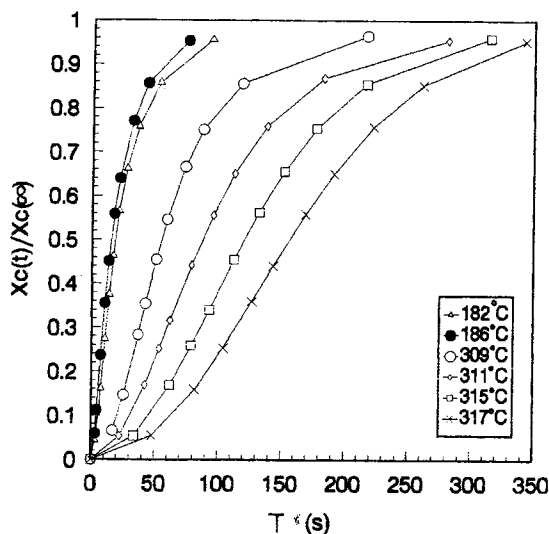


**Figure 5** The relative amount of degree of crystallization as a function of crystallization temperatures.

is the equilibrium melting temperature of PEEKK ( $T_m^0 = 387 + 273 = 660$  K).  $\Delta T$  is the degree of undercooling. It may be written as  $\Delta T = T_m^0 - T$ ,  $T_\infty = (T_g - 51.6)$ ,<sup>9,13</sup>  $f = 2T/(T_m^0 + T)$ .  $K_g$  contains the surface free energy product  $\sigma\sigma_e$ , the thickness  $b$  of the monomolecular layer on the growth face, and the heat of fusion of the perfect crystal  $\Delta H$ . The relationship to the linear growth rate  $G$  and Avrami parameter  $k$  can be written as

$$G \propto k^{1/n} \quad (7)$$

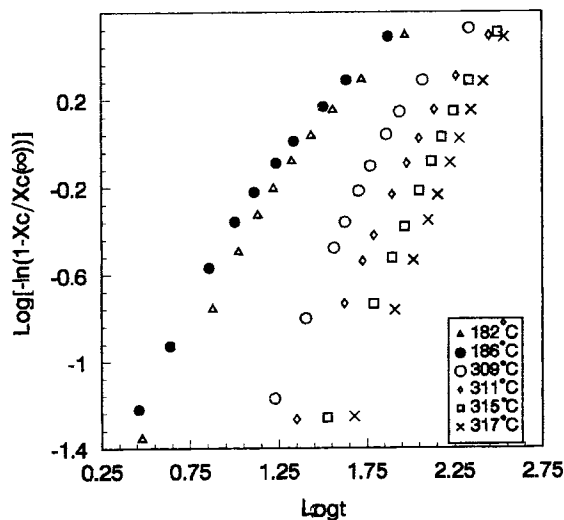


**Figure 6** The relationship between  $\log\{-\ln[1 - X_c(t)/X_c(\infty)]\}$  and  $\log t$  for isothermal crystallization from the melt and rubbery state.

**Table IV** Parameters  $n$  and  $k$  from the Avrami Analysis of Isothermal  $t_i$  Calculated from Eq. (4)

$T_c$ (°C)	$n$	$k$	$t_i$
309	2.01	$2.32 \times 10^{-4}$	0.76
311	1.90	$1.47 \times 10^{-4}$	1.17
315	1.99	$4.98 \times 10^{-5}$	1.71
317	2.13	$1.43 \times 10^{-5}$	2.33
182	1.56	$1.07 \times 10^{-2}$	0.20
186	1.36	$1.31 \times 10^{-2}$	0.15

According to the combining of eqs. (5) and (7), we can get  $\ln G = -U/R(T - T_\infty) + \ln G_0 - K_g T_m^0 / T \Delta T$ . The graphs of  $[\ln G + U/R(T - T_\infty)]$  versus  $(fT\Delta T)^{-1}$  can be shown in Figure 7.  $K_g$  is obtained according to the slope of the curve in Figure 7, so we get the kinetic parameter of PEEKK at the high temperature (309–317°C); the value is about 851.1 K. Cebe and Hong<sup>9</sup> get the PEEK kinetic parameter in the same method under the similar crystallization temperature (306–315°C). Blundell and Osborn<sup>13</sup> calculated the PEEK kinetic parameter by using growth rate data derived from measurement of the average spherulite diameter. The values are, respectively, 660 K and 590 K. The kinetic parameter of PEEK is smaller than PEEKK, the thickness  $b$  of the monomolecular layer of PEEK is equivalent to that of PEEKK because of the same preferred growth face<sup>13,22</sup> and spacing,<sup>1,22</sup> and the crystallization surface free energy ( $\sigma\sigma_e$ ) of PEEK is also lower than that of PEEKK; therefore, we think the crystallizability of PEEK is better than PEEKK.<sup>23,24</sup> This can be explained by the molecular

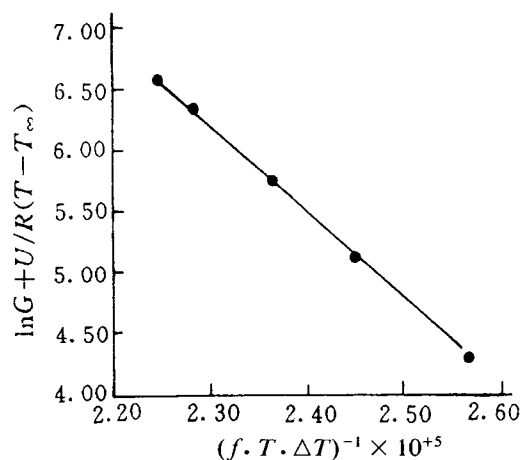


**Figure 7** Plot of  $[\ln G + U/R(T - T_\infty)]$  vs.  $(fT\Delta T)^{-1}$  for isothermal crystallization of PEEKK.

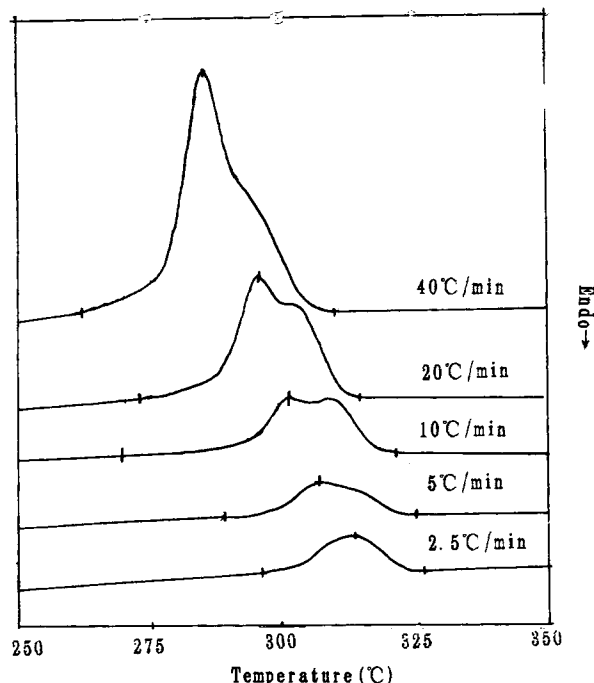


**Figure 8** Heat flow vs. temperature during nonisothermal crystallization of PEEKK cooled from the melt.

structure of PEEKK, because the PEEKK molecular main chain is increased by a benzoyl group. This destroys the degree of perfection of the molecular chain, and the crystallizability of PEEKK is weaker than that of PEEK. In addition, Jog and Nadkarni got the similar conclusions by the studies of the crystallization kinetics of PEKs.<sup>25</sup> The chain flexibility and mobility of PEKs are expected to decrease with the increasing ratio of ketone to ether linkages. Therefore, PEEK with a greater chain flexibility and mobility is more readily crystallizable than PEEKK.

#### Nonisothermal Crystallization Kinetics of PEEKK

Crystallization of PEEKK was also studied under nonisothermal conditions of cooling from 2.5°C/min to 40°C/min. The results are shown in Figure 8, the exothermic peak shifts to lower temperature as the cooling rate increases, and the peak shapes become more broad. At the highest cooling rate of 40°C/min, the peak occurs at a temperature of 285.6°C; at the lowest cooling rate of 2.5°C/min, the peak is 313.5°C. Values of temperature, time, and relative degree of crystallinity at maximum heat flow are listed in Table V. Integration of the exothermic peaks during the nonisothermal scan gives the relative crystallinity versus time; these results are shown in Figure 9. The inflection point,  $t_i$ , in each

**Table V** Temperature, Time, and Relative Crystallinity at Maximum Rate of Heat Flow During Nonisothermal Crystallization

Rate (°C/min)	Temperature $T$ (°C)	Time $t_i$ (min)	$X(t)/X(\infty)$
-40	286	0.61	0.61
-20	298	0.96	0.64
-10	301	2.01	0.66
-5	307	3.67	0.61
-2.5	313	6.29	0.61

curve represents the temperature corresponding to the maximum rate of heat flow. The relative degree of crystallinity at  $t_i$  during different cooling rates is relatively constant, ranging from 0.61 to 0.66. It is useful to compare the nonisothermal crystallization behavior of PEEKK with that of PEEK<sup>9</sup>; the inflection point  $t_i$  in each curve represents the time corresponding to the maximum rate of heat flow which can be used to compare the crystallization rate. Table VI presents the time at which PEEK and PEEKK reach the maximum heat flow. At the same cooling rate, the  $t_i$  of PEEKK is longer than that of PEEK<sup>9</sup>; in addition, Table VI also includes two kinds of degrees of undercooling; one is the difference between the melting point and the temperature at which the maximum heat flow is reached, the other is the value of the melting point minus the onset temperature of crystallization. From Table VI, we see that  $t_i$ , two kinds of degree of undercooling of PEEKK, are larger than those of PEEK and sug-

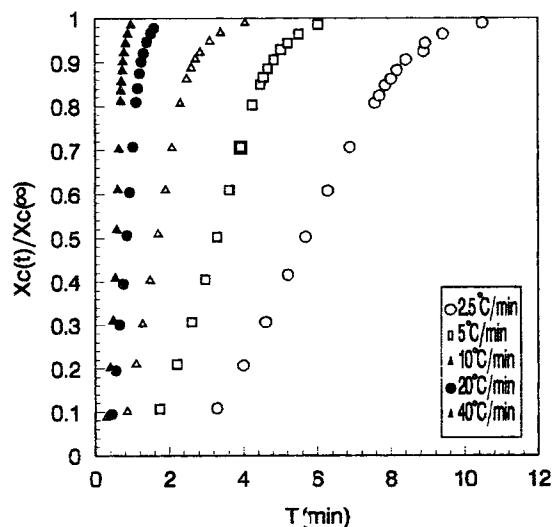


**Figure 9** Relative crystallinity vs. time during nonisothermal crystallization at different cooling rates.

**Table VI**  $t_i$  and Two Kinds of Undercooling Degrees of PEEKK and PEEK at Different Cooling Rates

Cooling Rate (°C/min)	PEEKK			PEEK		
	$T_m - T_{on}$ (°C)	$T_m - T_i$ (°C)	$t_i$ (min)	$T_m - T_{on}$ (°C)	$T_m - T_i$ (°C)	$t_i$ (min)
-20	44.9	64.2	0.96	41.0	50.0	0.50
-10	38.8	58.9	2.01	34.0	42.1	0.89
-5	34.8	53.2	3.67	29.0	37.0	1.63

$T_m$ , melting point;  $T_i$ , temperature which compound reaches the maximum heat flow;  $T_{on}$ , onset temperature of crystallization;  $t_i$ , time which compound reaches maximum heat flow.

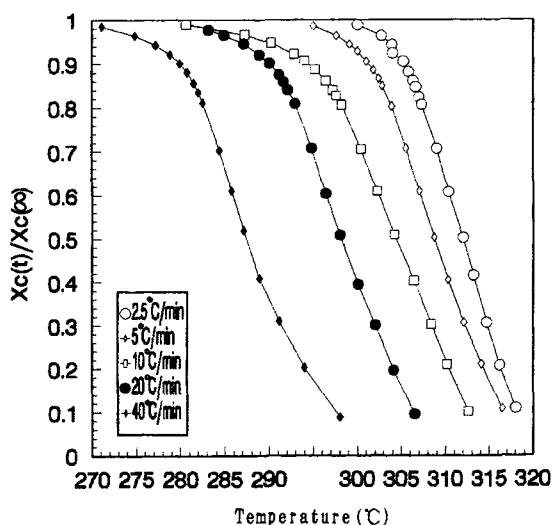
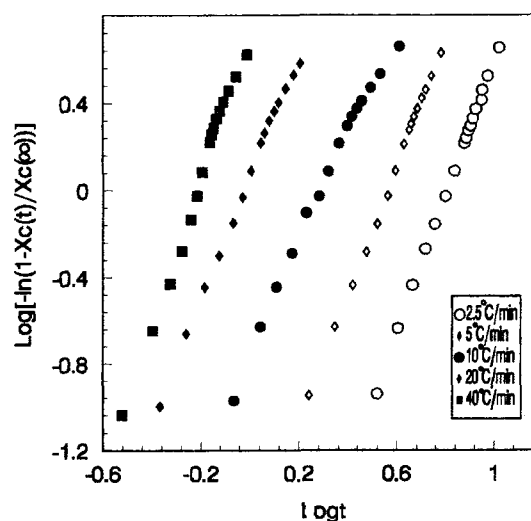
gest that the crystallization rate of PEEK is slightly faster than that of PEEKK in the nonisothermal crystallization condition. The nonisothermal crystallization is somewhat similar to the isothermal crystallization. The relative degree of crystallinity increases as the temperature decreases. Figure 10 presents the changing conditions: first there is a fast primary stage, followed by a slow secondary process. Crystal nucleation and growth parameters are dependent on temperature. Regarding the nonisothermal crystallization, we can analyze it with the Mandelkern method<sup>4</sup>; this is a modification of the Avrami equation. The crystallization temperature is supposed to be a constant. We can apply the Avrami equation to the nonisothermal kinetics. Values of  $n$  and  $k$  were determined for the nonisothermal kinetic data from the Avrami equation  $1 - X(t) = \exp(-Z_t t^n)$  or

$$\log[-\ln(1 - X(t))] = \log Z_t + n \log t \quad (8)$$

where  $X(t)$  [ $X(t) = X_c(t)/X_c(\infty)$ ] is degree of conversion,  $Z_t$  is the crystallization rate constant,  $t$  is the crystallization time  $t = (T_0 - T)/R$ , and  $n$  is the Avrami parameter under the nonisothermal crystallization state. We can regard the cooling rate  $R$  as a correct function when we consider the particularity of nonisothermal crystallization kinetics. Then the crystallization rate constant can be approximately written as

$$\log Z_c = \log Z_t/R \quad (9)$$

The plots of  $\log\{-\ln[1 - X(t)]\}$  versus  $\log t$  under nonisothermal crystallization are shown in Figure 11, according to the experimental values, fitting the initial linear portion of each curve. The Avrami pa-

**Figure 10** Relative crystallinity vs. temperature during nonisothermal crystallization at different cooling rates.**Figure 11** Plot of  $\log\{-\ln[1 - X(t)/X(\infty)]\}$  vs.  $\log t$  for nonisothermal crystallization of PEEKK.



**Table VII Avrami Parameter,  $n$ , and Rate Constants  $Z_t$ ,  $Z_c$ , During Nonisothermal Crystallization of PEEKK**

Rate (°C/min)	$n$	$Z_c$	$Z_t$
-40	3.08	1.034	3.773
-20	2.81	1.006	1.137
-10	2.92	0.838	0.171
-5	2.94	0.466	0.0219
-2.5	3.14	0.097	0.0029

parameter,  $n$ , rate constant,  $Z_t$ ,  $Z_c$  can be calculated and shown in Table VII.  $Z_t$  and  $Z_c$  decrease with the decreasing of the cooling rate under the nonisothermal crystallization; the value of  $n$  is about 3, larger than those determined by the isothermal crystallization. Nonisothermal crystallization is different from isothermal crystallization of PEEKK. This is the result of the different crystallization rate under the nonisothermal crystallization process.

## CONCLUSIONS

When PEEKK crystallizes from the amorphous state, it usually shows two melting peaks. The upper melting peaks arise first and the lower melting peaks are developed later; the upper melting peaks shown in DSC thermograms are the combination of three parts: initial crystals formed before scanning, reorganization, and the melting–recrystallization of lower melting peaks in the DSC scanning period.

In the study of isothermal crystallization kinetics, the Avrami constant  $n$  is about 2 for PEEKK from the melt and 1.5 for PEEKK from the rubbery amorphous state. According to the Lauritzen–Hoffman equation, the kinetic parameter of PEEKK from the melt is 851.5 K, which is higher than that of PEEK and suggests the crystallizability of PEEKK is less than PEEK.

The study of crystallization on PEEKK under nonisothermal conditions is also reported for cooling rates from 2.5°C/min to 40°C/min, according to the comparison with PEEK, and deduces that the crystallization rate of PEEKK is slightly slower than of PEEK. The nonisothermal condition is studied by the Mandelkern analysis. The nonisothermal crystallization is different from the isothermal crystallization. This is due to the different crystallization rates under nonisothermal crystallization processes.

## REFERENCES

1. H. J. Zimmermann and K. Könnecke, *Polymer*, **32**, 3162 (1991).
2. K. Könnecke, *Angew. Makromol. Chem.*, **198**, 15 (1992).
3. K. Könnecke, *J. Macromol. Sci. Phys.*, **B33**, 37 (1994).
4. L. Mandelkern, *Crystallization of Polymers*, McGraw-Hill, New York, 1964, p. 254.
5. G. Heinz, R. R. Lieder, and J. Koch, European Patent O 327 984 A<sub>2</sub> (1989).
6. T. E. Attwood, P. C. Dawson, J. L. Freeman, L. R. J. Hoy, J. B. Rose, and P. A. Staniland, *Polymer*, **22**, 1096 (1981).
7. P. J. Holdsworth and A. T. Jones, *Polymer*, **12**, 195 (1971).
8. R. C. Roberts, *J. Polymer Sci.*, **B8**, 381 (1970).
9. P. Cebe and S. D. Hong, *Polymer*, **27**, 1183 (1986).
10. A. M. Jonas, T. P. Russell, and D. Y. Yoon, *Polymer preprints*, **36**(1), 320 (1995).
11. D. C. Bassett, R. H. Olley, and I. A. M. Al Raheil, *Polymer*, **29**, 1745 (1988).
12. S. Z. D. Cheng, M. Y. Cao, and Wunderlich, *Macromolecules*, **19**, 1868 (1986).
13. D. J. Blundell and B. N. Osborn, *Polymer*, **24**, 953 (1983).
14. D. J. Blundell, *Polymer*, **28**, 2248 (1987).
15. Y. Lee and R. S. Porter, *Macromolecules*, **20**, 1336 (1987).
16. Y. Lee and R. S. Porter, *Macromolecules*, **22**, 1756 (1989).
17. H. L. Chen and R. S. Porter, *J. Polym. Sci., Polym. Phys. Ed.*, **31**, 1845 (1993).
18. J. S. Chung and P. Cebe, *J. Polym. Sci. Part B: Polymer Physics*, **30**, 163 (1992).
19. M. Avrami, *J. Chem. Phys.*, **7**, 1103 (1939); *ibid*, **8**, 212 (1940); *ibid*, **9**, 177 (1941).
20. J. D. Hoffman and J. I. Weeks, *J. Res. Nat. Bur. Std., Sec. A*, **66**, 13 (1962).
21. J. I. Lauritzen, Jr. and J. D. Hoffman, *J. Appl. Phys.*, **44**, 4350 (1973).
22. Shanger Wang, Junzuo Wang, Tianxi Liu, Zhishen Mo, Hongfang Zhang, Decai Yang, and Zhongwen Wu (Submitted to publish).
23. Yan Chen, Junzuo Wang, Junkui Cao, Hui Na, and Zhongwen Wu, *Chemical Journal of Chinese Universities (China)*, **13**(2), 322 (1995).
24. Junkui Cao, Junzuo Wang, Yang Chen, and Zhongwen Wu, *Journal of Applied Polymer Science* (in press).
25. J. P. Jog and V. M. Nadkarni, *Journal of Applied Polymer Science*, **32**, 3317 (1986).

Received November 17, 1995

Accepted March 19, 1996